Bias Dependent Boolean Multivalue Logic Application of Resonant Tunneling Bipolar Transistors

A. Matiss, J. Driesen, S. Ehrich, W. Prost, F.-J. Tegude

Department of Solid State Electronics, University Duisburg-Essen
Lotharstrasse 55 (ZHO), D-47057 Duisburg, Germany
matiss@hlt.uni-duisburg.de

***Abstract* — Resonant tunneling diodes (RTD) are well suited for future digital circuit components. Their negative differential resistance (NDR) allows to reduce the logic depth and the number of devices required for logic circuits. The resonant tunneling bipolar transistor (RTBT) is a concept that exploits the NDR-property of the RTD and the functionality of a single heterostructure bipolar transistor (SHBT). The nonlinear behavior allows the realization of up to six different Boolean functions by using a single device only. The diversity of the Boolean functions is based on the DC offset of the input voltage applied to the RTBT.**

I. Introduction

III-V semiconductor devices have distinct advantages concerning very high frequency digital and analog applications, e.g. the high carrier mobility and the compatibility to widely used optical wavelengths for combined optical and electronic applications.

The **R**esonant **T**unneling **D**iode (RTD) has demonstrated high potential regarding high speed, multiple-valued digital applications [1,3]. This device allows to build up rather complex digital gates with quite a small number of elements, and therefore with a minimum of space on the die [6].

Well known RTD circuits are the MOBILE (**Mo**nostable **Bi**stable Transition **L**ogic **E**lement) structures where at least two RTDs are combined, together with switching elements like HFET, MODFET or HBT devices [5]. The combination of switching transistors and RTD results in monolithically integrated devices, where the transistor and the RTD have been merged into a new device. One of these results is the **R**esonant **T**unneling **B**ipolar **T**ransistor, RTBT [2].

The investigations described in the subsequent sections concern the modeling and measurement of the most simple gate circuit possible with these devices. Especially the bias dependent gate functionality is demonstrated and the DC and RF model of the device is validated by comparing not only single device characteristics but also time domain gate measurements with corresponding simulations.

II. Device Technology

Basically the RTBT consists of a HBT with a RTD incorporated in the HBT emitter. We started the fabrication of the demonstrator circuits with the growth of the RTD/SHBT layer stack by metal-organic vapor phase epitaxy (MOVPE). The experiments were done on (001)±0.5° orientated s.i. InP:Fe epi-ready substrates in an AIX200-system with rf-heating at p_{tot}= 50 mbar reactor pressure using N_2 carrier gas. A non-gaseous-sources (ngs-) configuration is used based on TBAs/TBP/TMAs as group-V, DitBuSi/CBr_4 as group-IV n-/p-type dopant sources, and the metalorganics TMIn/TEGa. [7].

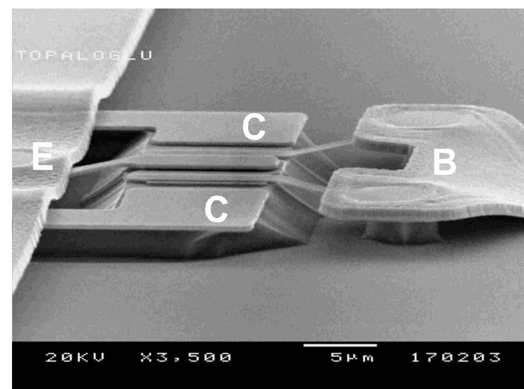

Fig. 1: SEM image of RTBT

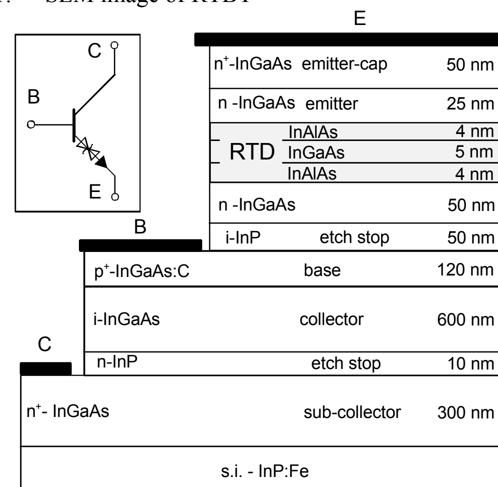

Fig. 2: Layer system of the used RTBT

A mesa technology is applied using wet chemical etching. Non-alloyed ohmic contacts are realized with Ti/Au metallizations for emitter and collector and Pt/Ti/Pt/Au for the base. To reduce parasitic capacitances the contacts of the devices are placed on extra mesas connected to the inner devices via underetched airbridges. Further details on RTD/HBT processing are described by W. Otten et al. [4].

III. Device Characterization

All measurements have been performed using an on-wafer measurement setup. First of all, the Single

Heterojunction Bipolartransistor has been characterized by measuring the DC and RF characteristics. The standard I-V-curves (output characteristics, Gummel plots, diodes and more) have been used to extract the bulk resistances, saturation currents, ideality factors and current gains.

For the RTBT, the additional RTD characteristic in the BE diode has to be taken into account. This results in a negative differential resistance regime in the output characteristics as shown in Fig. 3. Therefore, V_{BE} voltages in excess of 1.3 V have to be applied to extract the R_E bulk resistance. In order to analyze the specific properties of the RTBT, separate SHBT and RTD as reference structures have been realized.

The figures of merit for high frequency performance are the transit frequency f_T and the maximum frequency of oscillation f_{max}. These values are $f_T = 70$ GHz and $f_{max} = 83$ GHz in case of the SHBT at $V_{CE} = 1.8$ V and $I_B = 250$ µA, and $f_T = 45$ GHz and $f_{max} = 40$ GHz for the RTBT at the same bias conditions.

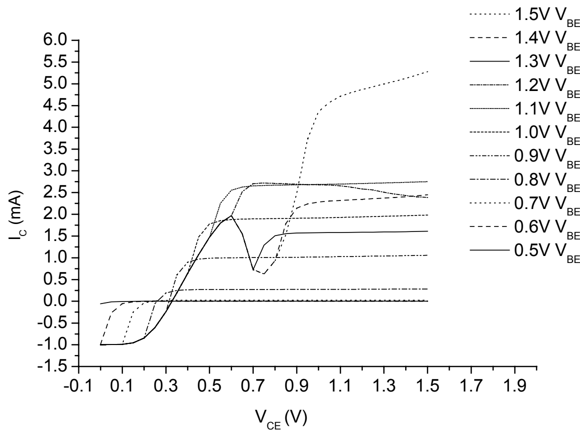

Fig. 3: Measured V_{BE}-controlled output-characteristic of one RTBT showing the envelope of the RTD-I/V characteristic

IV. RTBT-Modeling

The RTBT model used in this investigation is a series connection of the SHBT model and the additional RTD model in the emitter. Furthermore, parasitic elements have been added. The complete model is shown in fig. 4.

For the HBT the standard Gummel-Poon model is used. The equivalent circuit describing the RTD is given in fig. 5. The mathematical description of the voltage controlled current source is based on five currents, each switched on and off in the specific regions of the I-V curves using the tanh function. The parameters are all fitted to the measured curves.

$$I_{RTD}(U_{RTD}) = F \cdot (i_{peak} \cdot l_P(U_{RTD}) + r_P(U_{RTD}) - l_n(U_{RTD}) - r_n(U_{RTD}) + itherm \cdot idt(U_{RTD}))$$

$$l_P(U_{RTD}) = \frac{1}{2} \cdot \exp\left(\frac{-(U_{RTD} - U_{resp})^2}{W_{rl}^{\,2}}\right) \cdot (1 - \tanh(10(U_{RTD} - U_{resp})))$$

$$r_P(U_{RTD}) = \frac{1}{2} \cdot \exp\left(\frac{-(U_{RTD} - U_{resp})^2}{W_{rr}^{\,2}}\right) \cdot (1 - \tanh(10(U_{RTD} - U_{resp})))$$

$$l_n(U_{RTD}) = \frac{1}{2} \cdot \exp\left(\frac{-(-U_{RTD} + U_{resn})^2}{W_{rl}^{\,2}}\right) \cdot (1 - \tanh(10(-U_{RTD} + U_{resn})))$$

$$r_n(U_{RTD}) = \frac{1}{2} \cdot \exp\left(\frac{-(-U_{RTD} + U_{resn})^2}{W_{rr}^{\,2}}\right) \cdot (1 + \tanh(10(-U_{RTD} + U_{resn})))$$

$$idt(U_{RTD}) = \exp(de \cdot U_{RTD}) - \exp(-de \cdot U_{RTD})$$

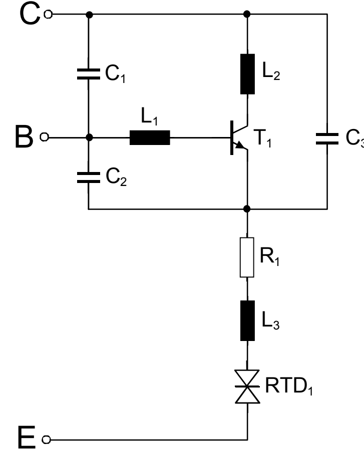

Fig. 4: Equivalent circuit of the RTBT consisting of the rf-environment (C_1, C_2, C_3, L_1, L_2, and L_3) the transistor T_1 and the RTD

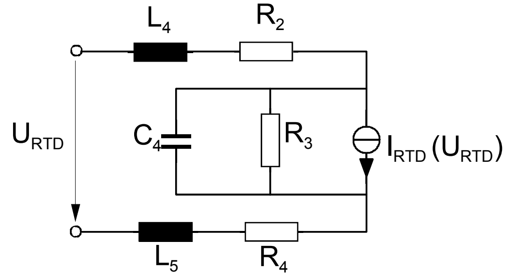

Fig. 5: Equivalent circuit of the RTD consisting of the rf-environment (L_4, L_5, C_4, R_2, R_3 and R_4) and the voltage controlled current-source I_{RTD}

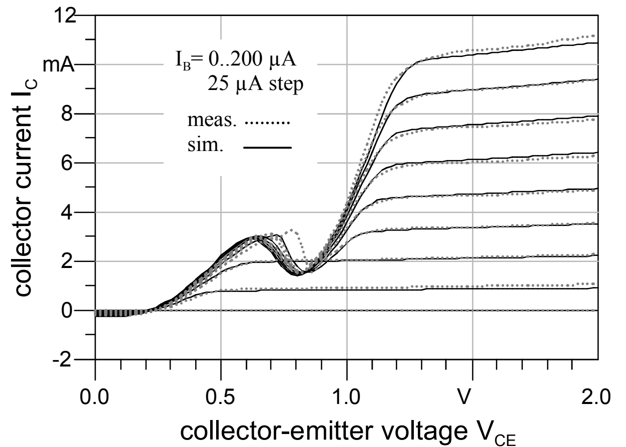

Fig. 6: Simulated and measured common emitter output characteristic.

Good agreement between measured and modeled data in case of the common emitter output characteristics is achieved, as well as acceptable agreement for the RF behavior, represented by the s-parameters near "peak-current" (fig. 7) and well above the NDR regime (fig. 8).

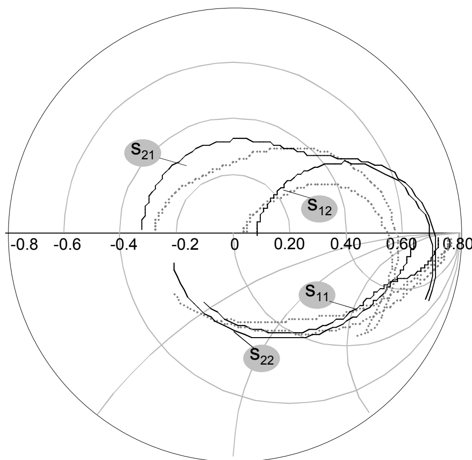

Fig. 7: Measured (dotted) and modeled (solid) s-parameters at $V_{CE} = 0.6V$ and $I_B = 50\mu A$, at the peak current.

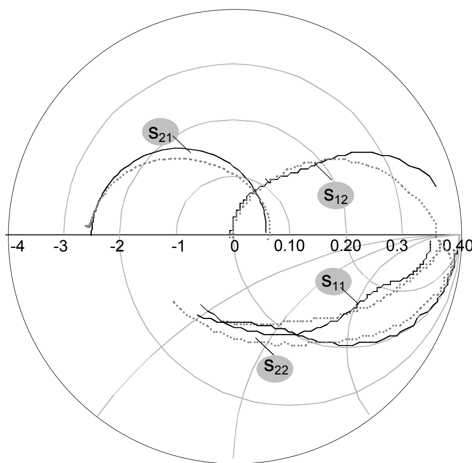

Fig. 8: Measured (dotted) and modeled (solid) s-parameters at $V_{CE} = 1.8V$ and $I_B = 250\mu A$, above the NDR regime.

MULTIFUNCTIONAL BOOLEAN LOGIC

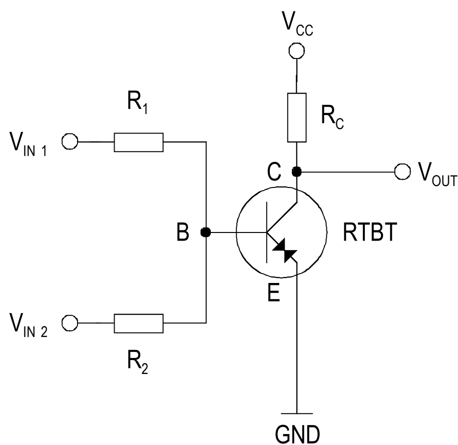

Fig. 9 Schematic circuit of the multivalue logic gate

The RTBT forms a the multiple valued logic gate with a resistive network R_1, R_2 and a load resistor R_C. Two binary inputs with equal high/low voltages allow the realization of up to three different voltage levels at the base terminal of the RTBT. This results in up to six different logic functions if both inputs are driven with equal signal levels. The load resistor defines the output signal levels. The V_{CC} bias voltage adjusts the output offset level.

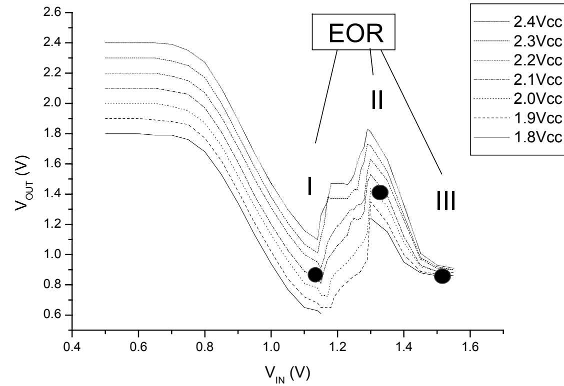

Fig. 10 Transfer characteristic of the gate for different bias voltages V_{CC} (EOR operation points are marked)

The gate transfer characteristic can be adjusted by V_{CC} to achieve a sufficient output voltage level necessary to drive a next stage in a logic circuit.

The logic function is set by an offset voltage additional to the signal voltage amplitude of the two input terminals. V_{CC} has to be adjusted to exploit the negative differential region of the RTD. For $V_{CC} > 1.8V$ the NDR property is valid. Above this level six logical functions can be realized (Fig. 10, Tab. 1). By choosing the proper bias voltage V_{CC} and load resistor R_C the output voltage V_{out} will maintain the same voltage level for two different input voltages (e.g. I and III; see. Fig. 10). These operation points are usually located around the peak (I) or valley (II) currents of the RTD and four logic functions can be realized (NAND, NOR, EOR, ENOR). Two more functions have an operation point in the negative resistance region to achieve a constant output voltage for two input voltages. These are the AND and the OR function.

V. MEASUREMENT SETUP

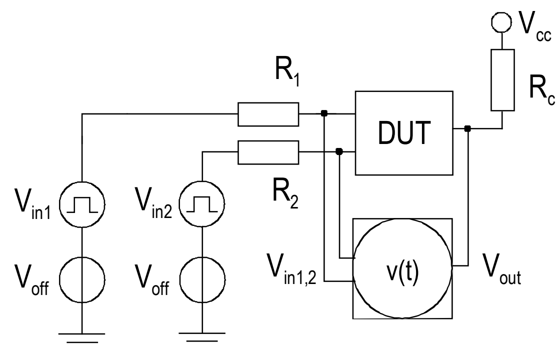

Fig. 11 Measurement setup for the verification of logical functions with a single resonant tunneling bipolar transistor

For the verification of the logic functions the measurement setup presented in fig. 11 is used. To perform measurements on devices without any buffer stages, a low-frequency real-time oscilloscope (DC to 500MHz) with an input impedance of 1 MΩ has been employed to record the input and output voltages. To provide the proper input voltages, a 3.35 GHz pulse/square generator with two outputs is connected to

an on-wafer resistance network. One channel is phase shifted by 90° to provide all possible combinations of the two input signal during one period. The resistance network R_1 and R_2 consists of two 100Ω resistors as shown in fig. 11. A Microwave probe station provides a coaxial to co-planar conversion to create a connection to the input and output of the RTBT-circuit on the wafer. An additional third probe applies the bias V_{CC} to the load resistance R_C in the collector branch. The recorded signals are the output signals of the generator, which shows the two resulting phase-shifted signals, and the output voltage at the collector. The frequency range was limited by the circuit-design and also by the oscilloscope bandwidth, so measurements have been performed up to 150 MHz source frequency. The different measurements are made by only adjusting the input voltage levels and offsets to fit the requirements of the respective logic function. The bias voltage as well as the resistances are kept constant (R_C = 100Ω, $R_{1,2}$ = 100Ω, V_{CC} = 2.1 V).

VI.. Measurement Results

This section presents the measurement results with a detailed table of all Boolean functions verified with the previously described circuitry.

Function	$V_{in1,2}$		V_{out}		
	(L)ow	(H)igh	$V_{in1,L}=V_{in2,L}$	$V_{in1} \neq V_{in2}$	$V_{in1,H}=V_{in2,H}$
NAND	0.3V	1.1V	H (2.1V)	H (2.1V)	L (1.2V)
NOR	0.7V	1.5V	H (1.9V)	L (1.0V)	L (1.0V)
EOR	1.1V	1.5V	L (0.95V)	H (1.4V)	L (0.95V)
ENOR	0.9V	1.3V	H (1.3V)	L (1.0V)	H (1.3V)
AND	1.03V	1.33V	L (1.1V)	L (1.1V)	H (1.4)V
OR	1.1V	1.4V	L (0.95V)	H (1.2V)	H (1.2V)

Tab. 1 Boolean operation voltages of input and output for different functions. (R_C=100 Ohm, $R_{1,2}$=100 Ohm, V_{CC}=2.1V)

The functions have been verified for different bias conditions (Tab. 1). Two of the six time-domain signals are shown in fig. 12 and 13 demonstrating the two functions AND and EOR.

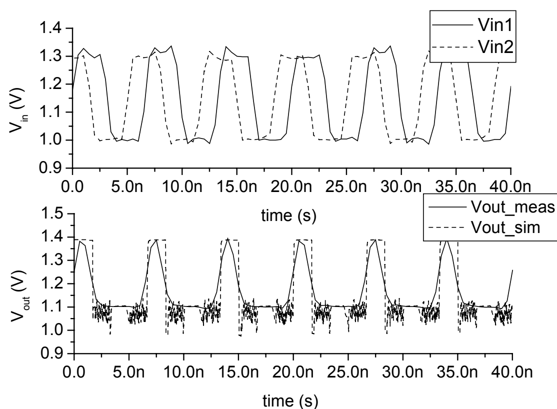

Fig. 12 Comparison of simulated and measured results for the AND-function

In the simulation, the AND function shows oscillating behavior in the NDR operation point as observed in fig. 12. The oscillation could not be observed during the measurement due to the limited bandwidth of the oscilloscope of 500 MHz. Therefore the output voltage appears to be constant for the low-level within the measurement range. A good agreement for the EOR function between the simulated results and the measurement results is presented in fig. 13. Small variations between the simulated and measured plots are partly due to the limited amount of obtained measurement points which do not allow a good interpolation of the real waveform at the investigated frequency.

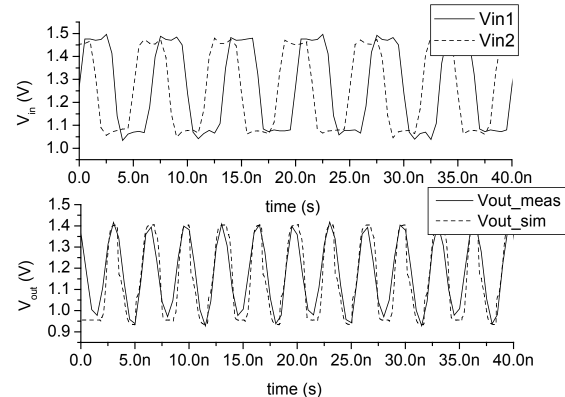

Fig. 13 Simulated and measured results of the EOR function

VII. Conclusion

The combination of the resonant tunneling diode in the emitter branch of a heterostructure bipolar transistor yields advantages in device count per function for future logic design. Based on Boolean input and output logic, six different logic function have been verified using a single device and only adjusting the DC-bias voltages, which makes them suitable for digital applications.

References

[1] P. Mazumder, S. Kulkarni, M. Bhattacharya, J. Ping Sun, G. I. Haddad: *Digital Circuit Applications of Resonant Tunneling Devices,* Proceedings of the IEEE, VOL. 86, NO. 4, April 1998

[2] F. Capasso, et Al.: Quantum Functional Devices: *Resonant-Tunneling Transistors, Circuits with Reduced Complexity, and Multiple-Valued Logic*, IEEE Transactions on Electron Devices, VOL. 36. NO. 10, October 1989

[3] H. I. Chan, S. Mohan, P. Mazumder, G. I. Haddad: *Compact Multiple-Valued Multiplexers Using Negative Differential Resistance Devices*, IEEE Journal of Solid-State Circuits, VOL. 31, NO. 8, August 1996

[4] W.Otten, P.Glösekötter, P.Velling, A.Brennemann, W.Prost, K.F.Goser, F.J.Tegude; *InP-based monolithically integrated RTD/HBT MOBILE for logic circuits*, Proc. 13th InP & Related Materials Conf., pp. 232-235, 2001.

[5] S. Choi, B. Lee, T. Kim and K. Yang: *CML-type Monostable Bistable logic element (MOBILE) using InP-based monolithic RTD/HBT technology*, Electronic Letters, VOL. 40. NO. 13, 24th June 2004

[6] C.H. Lin, K. Yang, et Al.: *Monolithically Integrated InP-based Minority Logic Gate Using an RTD/HBT Heterostructure*, 10th Intern. Conf. On Indium Phosphide and Related Materials, 11-15 May, 1998, Tsukuba, Japan

[7] P. Velling, M. Agethen, W. Prost ,F.J. Tegude: *InAlAs/InGaAs/InP Heterostructures for RTD and HBT Device Applications Grown by LP-MOVPE Using Non-Gaseous Sources*, Journal of Crystal Growth, Japan, June 2000, pp. 722-729